

RECLAMATION

Managing Water in the West

Technical Report No. SRH-2014-31

Modeling of Delta Erosion during Elwha Dam Removal with SRH-2D



U.S. Department of the Interior
Bureau of Reclamation
Technical Service Center
Denver, Colorado

September 2014

Mission Statements

The mission of the Department of the Interior is to protect and provide access to our Nation's natural and cultural heritage and honor our trust responsibilities to Indian tribes and our commitments to island communities.

The mission of the Bureau of Reclamation is to manage, develop, and protect water and related resources in an environmentally and economically sound manner in the interest of the American public.

Technical Report No. SRH-2014-31

Modeling of Delta Erosion during Elwha Dam Removal with SRH-2D

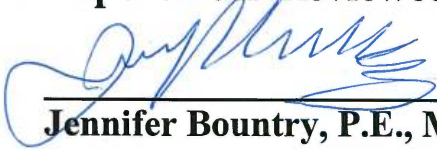
Prepared by:



Yong G. Lai, Ph.D., Hydraulic Engineer
Sedimentation and River Hydraulics Group, Technical Service Center

9-30-2014
Date

Report Peer Reviewed by:



Jennifer Bountry, P.E., M.S., Hydraulic Engineer
Sedimentation and River Hydraulics Group, Technical Service Center

9-30-2014
Date



U.S. Department of the Interior
Bureau of Reclamation
Technical Service Center
Denver, Colorado

September, 2014

Table of Contents

	Page
Executive Summary	1
1.0 Introduction.....	3
2.0 Description of SRH-2D Model	5
2.1 General Description	5
2.2 Bank Erosion Modules.....	6
2.2.1 Basal Erosion	6
2.2.2 Uniform Retreat Module.....	7
2.2.3 Mechanistic Failure Module	8
2.2.4 Basal Cleanout Module	9
2.2.5 Coupling Procedure	10
2.2.6 Solution Flow and Data Exchange.....	13
3.0 Model Verification	15
4.0 Results with Glines Canyon Dam Removal Physical Model Scenario	25
4.1 About the Physical Model Test.....	25
4.2 Case 3xC Scenario	28
4.3 Other Model Details.....	30
4.4 Model Results	34
5.0 Concluding Remark.....	41
6.0 References.....	42

Index of Figures

	Page
Figure 1. Diagram of bank retreat computation with the uniform retreat module..	8
Figure 2. Illustration of a channel reach for geofluvial modeling: right bank is subject to bank retreat.	11
Figure 3. Flume configuration and initial meander channel form	15
Figure 4. Initial meshes used for Run 1 and Run 3 using both the moving and fixed mesh approaches (contour represents the initial bed elevation)	17
Figure 5. Initial and final meshes for Run 1 with the moving mesh (contours are bed elevation).....	19
Figure 6. Comparison of predicted and measured bank retreat for Run 1	20
Figure 7. Initial and final meshes for Run 3 with the moving mesh (contours are bed elevation).....	21
Figure 8. Initial and final meshes for Run 3 with the mixed, moving mesh (contours are bed elevation).....	22
Figure 9. Comparison of predicted and measured bank retreat for Run 3.....	23
Figure 10. Contour map of pre-dam Elwha River valley showing locations of model construction cross-sections	27
Figure 11. Initial terrain and terrain after 220 minutes during the physical model test.....	28
Figure 12. Contours of the empty basin terrain and the initial delta terrain used for both numerical and physical models.....	29
Figure 13. Contours of the initial delta terrain used for the numerical modeling; note the entrance channel and the pilot channel added to the delta. Note that all elevations below 55 are shown as blue to emphasize topography in delta section.	30
Figure 14. Solution domain and mesh used for the simulation.....	32
Figure 15. Initial sediment gradation of the delta in the physical model test	33
Figure 16. Three boundary lines (shown in black) used to define bank erosion zones	33
Figure 17. 3D view of the initial geometry of the 3xC case.....	34
Figure 18. Predicted flow velocity and water depth for the flow-only model run (blank area in velocity plot is the almost still water area)	35
Figure 19. Predicted erosion and deposition depth (cm) of the delta when no dam removal is performed	36
Figure 20. Simulated delta evolution to equilibrium	38
Figure 21. Comparison of predicted (black dots are locations of the initial pilot channel) and measured erosion and deposition depth (cm) when the delta reached equilibrium after removal of 3 notches.....	39
Figure 22. Predicted erosion and deposition depth (cm) when the delta reached equilibrium after removal of 3 notches without bank erosion module turned on.	40

Index of Tables

	Page
Table 1. Prototype and model geometrical hydraulic variables.....	26
Table 2. Sediment size classes within the initial delta with the numerical model	31

Executive Summary

In this study, the geofluvial SRH-2D model, which coupled bank erosion modules with the mobile-bed model, is used to simulate the delta erosion and deposition characteristics when dam notches are removed in the physical model of Elwha Dam removal. The primary research question is whether the existing SRH-2D is capable of predicting both vertical and lateral sediment erosion and deposition processes experienced during dam removal. If not, what is needed in future development of the model.

The study reaches the following conclusions:

- Early in the research, some limitations of the model are found in that the model cannot be used to simulate the delta channel processes well. New modeling options and model improvements are developed in order to achieve the reported modeling results.
- With the new model, some success has been achieved in that the model is successfully used to simulate the simultaneous vertical and lateral erosion of the delta processes during dam removal. Qualitative erosion and deposition patterns are well predicted by the model. It is found that, without lateral bank erosion, the predicted erosion pattern is completely incorrect.
- The updated SRH-2D model still misses some of the details of the delta erosion. For example, predicted erosion at the upstream half of the pilot channel is not observed in the physical model.
- It is also found during the course of the study that the improved bank erosion modules implemented in SRH-2D still have rooms for improvement as the model may fail if the bank toe point moves significantly in the vertical direction.

It is recommended that further research and development are needed in the future. New bank module needs to be developed that can track the bank toe point in a robust and stable way.

1.0 Introduction

SRH-2D is a two-dimensional model developed by Dr. Yong Lai at the Bureau of Reclamation, Technical Service Center. It has been widely used for both hydraulic and sediment modeling for engineering projects since 2006. SRH-2D has been applied to simulate reservoir delta evolution upstream of the Robles Diversion Dam on the Ventura River, California (Lai and Greimann 2008). New bank erosion modules have also been developed by Dr. Lai to simulate both vertical and lateral stream erosion processes (Lai et al. 2014).

In this study, the new SRH-2D model including bank erosion modules was applied to simulate the delta processes during the removal of Glines Canyon Dam in the former Lake Mills on the Elwha River in Washington State. The primary research question of the study is whether the current SRH-2D is capable of predicting both vertical and lateral sediment erosion and deposition processes resulting from reservoir drawdown. As of 2014, the Elwha River restoration was the largest dam removal project in North America. Removal of two dams on the Elwha exposed roughly 24 million cubic yards of sediment and wood trapped in the reservoirs, the majority of which was in Lake Mills. Based on field experience in 1994 and laboratory modeling, both vertical and lateral sediment erosion processes were very important during the lowering of the reservoir (Childers et al, 2007; Bromley, 2007).

We utilized the unique in-kind data and opportunity posed from this unprecedented project to test SRH-2D and the incorporated bank erosion modules. Testing of the field drawdown case was accomplished by University of Arizona and is separately documented. In the following chapters, the SRH-2D model and bank modules are described; the model setup process, input parameters and model results are then reported when SRH-2D is used to predict the delta processes during dam removal under the physical model scenario.

2.0 Description of SRH-2D Model

2.1 General Description

SRH-2D, Sedimentation and River Hydraulics – Two-Dimensional model, is a 2D depth-averaged hydraulic and sediment transport model for river systems developed at the Bureau of Reclamation, Technical Service Center. The hydraulic flow modeling theory was documented by Lai Yong (2008; 2010). The model adopts the arbitrarily shaped element method of Lai et al. (2003), the finite-volume discretization scheme, and an implicit integration scheme. The numerical procedure is sufficiently robust that SRH-2D can simultaneously model all flow regimes (sub-, super-, and trans-critical flows) and both steady and unsteady flows. The special wetting-drying algorithm makes the model very stable in handling flows over dry surfaces. The mobile-bed sediment transport module adopts the methodology of Greimann et al. (2008). Theories have been described in the reports and papers by Lai and Greimann (2010) and Lai et al. (2011). The mobile-bed module predicts vertical stream bed changes by tracking multi-size, non-equilibrium sediment transport for suspended, mixed, and bed loads, and for cohesive and non-cohesive sediments, and on granular, erodible rock, or non-erodible beds. The effects of gravity and secondary flows on the sediment transport are accounted for by displacing the direction of the sediment transport vector from that of the local depth-averaged flow vector.

Major capabilities of SRH-2D are listed below:

- 2D depth-averaged solution of the dynamic wave equations for flow hydraulics;
- An implicit solution scheme for solution robustness and efficiency;
- Hybrid mesh methodology which uses arbitrary mesh cell shapes. In most applications, a combination of quadrilateral and triangular meshes works the best;
- Steady or unsteady flows;
- All flow regimes simulated simultaneously: subcritical, supercritical, or transcritical flows;
- Mobile bed modeling of alluvial rivers with a steady, quasi-unsteady, or unsteady hydrograph.
- Non-cohesive or cohesive sediment transport;
- Non-equilibrium sediment transport;
- Multi-size sediment transport with bed sorting and armoring;
- A single sediment transport governing equation for both bed load, suspended load, and mixed load;
- Effects of gravity and secondary flows at curved bends; and
- Granular bed, erodible rock bed, or non-erodible bed.

SRH-2D is a 2D model, and it is particularly useful for problems where 2D effects are important. Examples include flows with in-stream structures such as weirs, diversion dams, release gates, coffer dams, etc.; bends and point bars; perched rivers; and multi-channel systems. 2D models may also be needed if certain hydraulic characteristics are important such as flow recirculation and eddy patterns; lateral variations; flow overtopping banks and levees; differential flow shears on river banks; and interaction between the main channel, vegetated areas and floodplains. Some of the scenarios listed above may be modeled in 1D, but additional empirical models and input parameters are needed and extra calibration must be carried out with unknown accuracy.

2.2 Bank Erosion Modules

New bank erosion modules have been developed in recent years which were incorporated into SRH-2D. For a coupled bank and stream erosion modeling, a number of physical processes, along with the coupling procedure, need to be developed. Physical bank erosion processes included in the SRH-2D modules are basal erosion (uniform retreat module), mass failure process (mechanistic failure module), and basal cleanout (basal cleanout module); coupling procedure includes the data exchange and mesh management. Details have been documented by Lai et al. (2012a; 2012b) and Lai (2013). A brief description is provided next.

2.2.1 Basal Erosion

With SRH-2D, an arbitrary number of banks can be selected for simultaneous bank retreat modeling and be coupled with the main channel processes. Each bank may be represented by an arbitrary number of bank nodes for bank geometry definition. The bank nodes do not need to be the same as the 2D mesh. For each bank, toe and top nodes are identified in the list of bank nodes and also in the 2D mesh. A requirement is that the two bank nodes must match two nodes in the 2D mesh. At the top node, zero vertical or lateral erosion is assumed. At the toe node, vertical erosion, along with other fluvial variables, is predicted by the 2D mobile-bed module, while the basal erosion (lateral direction erosion) of the wetted bank face is computed using a semi-empirical excess shear stress equation expressed as:

$$\varepsilon_L = k \left(\frac{\tau}{\tau_c} - 1 \right) \quad (1)$$

where

- ε_L = lateral erosion rate (m s^{-1})
- k = erodibility coefficient (m s^{-1})
- τ = shear stress on the bank node (Pa)
- τ_c = critical shear stress (Pa)

Shear stress on the bank node is computed by SRH-2D at the channel node located at the toe. This equation introduced two empirical coefficients (critical shear stress and erodibility) that need to be determined. The basal erosion along the entire bank is computed using the above equation.

2.2.2 Uniform Retreat Module

With the uniform retreat module, the mass failure is computed, after basal erosion, as follows: The bank profile from user defined toe to top nodes is assumed to be a straight line at a user specified angle (e.g., at the angle of repose for a given sediment grain size) and the bank retreat is computed such that the total area (volume) of retreat equals the area computed by the basal erosion. Tests showed that the predicted bank retreat results are insensitive to the bank angle used and therefore, initial bank angles computed automatically by the model may also be used.

The bank retreat rate of the uniform retreat module may be derived to be expressed in analytical form with the above mass conservation requirement, along with the linear shear stress distribution assumption. Its derivation is described next. Consider a bank shown in Figure 1. The initial bank is $G'ABC$ ($G'AB$ is wetted and under water while BC is dry and above water), and ABC is the straight bank face at the angle of repose. A is bank toe node, C is bank top, B is the intersect point between the bank and water surface, and G' is the nearest mesh node in the stream adjacent to A . After a time period, erosion is assumed to occur: A is eroded vertically to A' and G' is to G ; they are computed by the 2D model. By adding the lateral erosion of the toe node, A' would move to its final position F . The new bank face after basal erosion would be $GFBC$ due to the linear assumption of the shear stress along AB . Now the new bank angle of FB exceeds the angle of repose; therefore, the bank material above B would “fail” to fill the toe area and a final bank face, with the angle of repose, would form. That is, $GDIE$ would be the final bank face. The intercept point D between the new bank and the vertical line of AA' may be above or below D' . In Figure 1 and the derivation below, D is assumed to be above D' . Under such a scenario, D is assumed to be the final toe location. Mass (or area) conservation requires the following to be true ($IBCE$ refers to the area contained within the polygon, etc.):

$$IBCE = GDIFD' \quad (2)$$

With some derivation, the bank retreat distance r_B (i.e., distance between C and E) may be computed by the following equation:

$$r_B = 0.5 \frac{(h_0 + \omega_v)(\omega_L + \frac{\omega_v}{\tan \alpha}) + |GD|\omega_v}{(H_0 + \omega_v) + 0.5|GD|\tan \alpha} \quad (3)$$

where

r_B = bank retreat distance (m)

h_0 = initial water depth at toe (m)

- H_0 = initial bank height (m)
- α = bank angle or angle of repose (-)
- ω_v = vertical toe erosion distance predicted by the 2D model (m)
- ω_L = lateral toe erosion distance computed by equation (m)
- $|GD|$ = horizontal distance between G and D (m)

The bank retreat distance r_b under the other scenario of D below D' may be similarly derived; the final form is the same as equation (3) by setting $|GD| = 0$. Further, under the scenario of deposition at bank toe A, the bank would intrude towards the stream. The bank intrusion distance has also been derived similarly, and the final rate expression is also similar to equation (3) and they are not repeated.

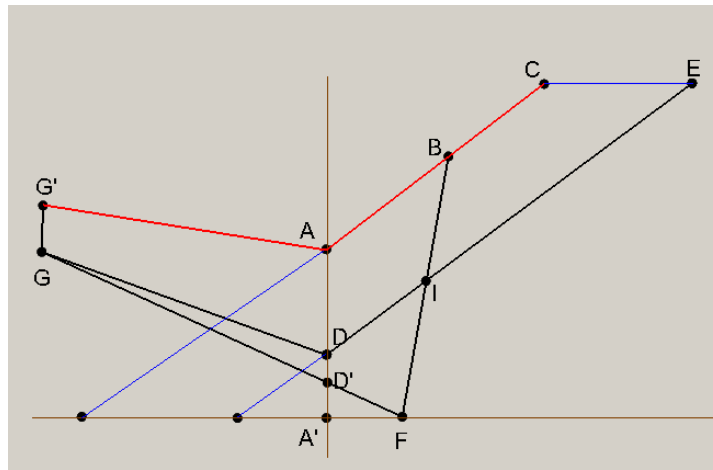


Figure 1. Diagram of bank retreat computation with the uniform retreat module

With the uniform retreat module, the entire bank is treated as “uniformly” retreating while the bank is eroded.

2.2.3 Mechanistic Failure Module

Basal erosion may erode a bank to a point that the bank is too steep to remain stable and a gravitationally-induced mass failure occurs. With the mechanistic failure module, a bank may consist of multiple layers and geotechnical mass failure is explicitly computed through process based models. The method follows the approach of Langendoen and Simon (2008), but with some important differences. Details have been presented by Lai et al. (2012b) and Lai (2013). The mechanistic failure module was developed in collaboration with the research team headed by Andrew Simon when he was employed by the National Sedimentation Laboratory (NSL), Agriculture Research Service. BSTEM, Bank-Stability and Toe-Erosion Model, was a product of NSL; a shortened and revised version was created so that it was appropriate to be incorporated into SRH-2D.

A bank may be represented by an arbitrary number of bank nodes (independent of 2D mesh nodes along the bank except the top and toe nodes), and it is assumed to consist of between one and an unlimited number of soil layers. Each bank layer may be assigned its own geotechnical properties. Basal erosion is carried out first and the computed lateral erosion is then applied to the bank profile. After basal erosion, the potential for mass failure is evaluated by first finding the base of the failure plane on the bank face and the angle of the failure plane. The failure plane is found through a search algorithm so that the block above the plane is the most unstable. Block stability is measured using the factor of safety, which is the ratio of resisting to driving forces, through a force equilibrium analysis. Mass failure occurs if the factor of safety is less than one; otherwise the bank is stable and no mass failure occurs.

The failure block is divided into many vertical slices for the stability analysis. The force equilibrium analysis is first carried out on each individual slice; the force balance of the entire failure is then obtained by summing all forces on the slices – an approach developed by Langendoen and Simon (2008). In SRH-2D, it is assumed that the groundwater table within the bank is horizontal as a constant elevation, pore-water pressures are distributed hydrostatically above and below the phreatic surface, and the bank is subject to planar or cantilever shear failures.

2.2.4 Basal Cleanout Module

Large chunks of soil blocks are often deposited at the bank toe following mass failure of cohesive banks. These blocks temporarily protect the bank from direct fluvial erosion, but over time are subject to subaerial weathering (when exposed) and gradual winnowing and eventual removal (when submerged). Many models ignored the bank toe protection features of the failed blocks, while others proposed a number of ways the impact be incorporated. With SRH-2D, basal cleanout was incorporated by placing failed materials into an invisible “tank” that has no topographic impact to the flow in the stream but is made available for preferential basal erosion by size fractions following mass failure. That is, the basal erosion process must erode the sediment in the tank according to each size classes first before the erosion of material in that size class from the wetted bank face is permitted. The tank approach explicitly accounts for the protection afforded by failed bank materials, does not make assumptions regarding the topographic form of failed blocks, and conserves the mass correctly. The use of an “invisible” tank removes the complexity needed to modify local bank geometry. However, the method ignores the impact of blocks on near-bank flow conditions which may lead to an underestimation of the erosion force. There are other processes that are ignored in the current implementation in SRH-2D such as weathering and the establishment and proliferation of vegetation. These processes may change the erodibility of the failed block. It is suggested that the ignored processes and other uncertainty be taken into consideration in the selection of the erodibility coefficient for basal erosion. Calibration of the erodibility coefficient is recommended for most practical applications.

2.2.5 Coupling Procedure

Strategy and procedures are needed on how to couple the bank modules with the 2D mobile-bed model. This is probably one of the most important steps in model development as stability and ease of use of the geofluvial model depend on them, particularly for time accurate continuous dynamic modeling. A general yet simple procedure is developed and used by SRH-2D.

The SRH-2D model input and setup procedure for a coupled geofluvial modeling is made very similar to that for a non-bank mobile-bed modeling. An initial 2D mesh is generated along with regular boundary conditions specified. With geofluvial modeling, an extra model setup is to add one or multiple bank segments to the 2D mesh so that each bank segment is represented by a block of mesh cells (named bank zone). Each bank segment is a bank zone on the 2D model and each may contain an arbitrary number of banks that require bank retreat modeling. As an illustration, Figure 2 shows a channel reach subject to geofluvial modeling whose right bank is to be simulated for bank retreat. Two bank segments are used in the example and each segment is represented with a bank zone consisting of 2D mesh cells. Bank zone 1 contains three banks, while zone 2 has four banks. Each bank zone is defined by two edge lines. With the moving mesh approach to be described next, one edge is along the bank toe and the other along the bank top. A one-to-one toe to top mesh line correspondence is assumed. With the fixed mesh approach, the two represent simply the beginning and ending edges of the bank zone. But the zone has to be wide enough so that both toe and top nodes are contained within the zone all the time.

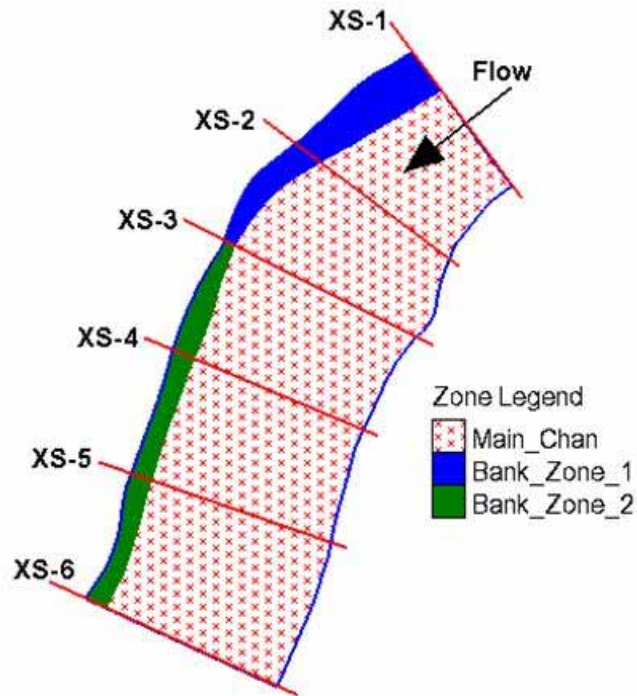


Figure 2. Illustration of a channel reach for geofluvial modeling: right bank is subject to bank retreat.

The above representation of banks on a 2D mesh is used only by the 2D mobile-bed module for computing appropriate flow hydraulics near the bank. Representation of each bank adopts a different method in which an arbitrary number of nodes may be used to describe the bank profile. The dual representations of a bank are used to improve the accuracy of bank retreat simulation. Large uncertainty may result if only the 2D mesh is used for bank representation since only a few 2D mesh points may be feasible to use for steep banks. Another benefit is that bank layering and geotechnical properties of each bank layer may be specified for each bank accurately, independent of the 2D mesh. Therefore, the dual representation strategy makes SRH-2D easy to use with geofluvial modeling, but with improved accuracy representing the bank properties and erosion quantities.

A key remaining issue is how to update the feedback between the morphological changes predicted by the bank module and the 2-D mobile-bed model during a continuous dynamic simulation. Two approaches are adopted by SRH-2D: the moving mesh and the fixed mesh approaches. The moving mesh approach adopts the Arbitrary Lagrangian-Eulerian (ALE) formulation of Lai and Przekwas (1994). With this approach, the longitudinal mesh lines are aligned with the bank toe and top initially. The bank line “alignment” is enforced continuously throughout bank retreat by moving the 2D mesh along with the bank. The moving mesh approach “captures” the bank lines, leading to a better bank representation and more accurate retreat computation. The main drawback is that the 2D mesh has to be remeshed over the simulation period whenever a bank is

moving, and the remeshing can only be done automatically by the model. The moving mesh approach has the potential to distort the mesh too much which can lead to model instability, particularly in areas with tight curves such as along the outside of meander bends. Therefore, moving mesh is the recommended model approach only if no significant bank retreat is expected, e.g., less than one channel width. The fixed mesh approach does not move the mesh in planform in response to erosion, deposition or bank retreat. With this approach, bank toe and top are found through a “fitting” (interpolation) procedure using nearby mesh nodes. Fixed mesh removes the mesh distortion issue, but bank toe and top are only approximately represented by the 2D mesh. The fitting may lead to high uncertainty that is proportional to the mesh density. Often, a much refined 2D mesh is required by the fixed mesh approach to capture bank retreat reasonably, increasing the computational time significantly. The fixed mesh method is recommended only if bank retreat is anticipated to be large (e.g., more than one channel width); and refined mesh should be used to reduce model uncertainty.

The fixed mesh approach requires tedious bookkeeping by the model, but is straightforward otherwise. The moving mesh approach is developed following the ALE formulation of Lai and Przekwas (1994). With this formulation, a mesh may be moved in an arbitrary manner. The governing equations are slightly modified from the fixed mesh formulation and they may be expressed in integral form for an arbitrarily moving mesh cell as:

$$\frac{d}{dt} \int_A h dA + \int_S h (\vec{V} - \vec{V}_g) \cdot d\vec{s} = 0 \quad (4a)$$

$$\frac{d}{dt} \int_A h \vec{V} dA + \int_S h \vec{V} (\vec{V} - \vec{V}_g) \cdot d\vec{s} = \int_S h \vec{\sigma} \cdot d\vec{s} + \int_A \vec{S}_v dA \quad (4b)$$

$$\frac{d}{dt} \int_A h \phi dA + \int_S h \phi (\vec{V} - \vec{V}_g) \cdot d\vec{s} = \int_S h \vec{q} \cdot d\vec{s} + \int_A S_s dA \quad (4c)$$

where

t = time (s)

h = water depth (m)

A = area (m²)

\vec{V} = fluid flow velocity vector (m/s)

\vec{V}_g = velocity vector of the moving mesh (m/s)

\vec{s} = edge length of a cell (m)

ϕ = a scalar variable that is being transport (ϕ)

$\vec{\sigma}$ = stress tensor (m²/s²)

\vec{q} = scalar flux vector (ϕ m/s)

\vec{S}_v = source/sink term of the momentum equation (m²/s²)

S_s = source/sink term of the scalar equation (ϕ m/s)

In the above, (4a) is mass conservation, (4b) is momentum conservation, and (4c) is for transport of a scalar (e.g., sediment concentration for each size class). Integration over A

denotes an arbitrary moving mesh cell, and over S is the side of the cell with the vector representing the unit normal. The grid velocity is computed using a geometric constraint, called the space conservation, written as:

$$\frac{d}{dt} \int_A dA = \int_S \vec{V}_g \cdot d\vec{s} \quad (5)$$

The procedure developed by Lai and Przekwas is used to compute the grid velocity accurately using equation (5). Once the grid velocity is computed, the discretization and solution algorithms are the same as the non-moving-mesh cases. With the ALE method, main flow and sediment variables represented by the mesh cells are automatically computed in a time-accurate manner; there is no need for additional interpolations except for derived variables such as bed topography.

2.2.6 Solution Flow and Data Exchange

The timescale of the bank retreat process is much longer than that of in-stream fluvial processes (hydraulic and sediment) and thus the time step of the bank module is generally much larger than the 2D mobile-bed model. In a typical simulation, the 2D mobile-bed modeling is carried out first assuming fixed banks; flow hydraulics and vertical bed changes are predicted. The mobile-bed modeling proceeds in its own time step until it reaches the bank time step to activate the bank module. The model then carries out the following steps:

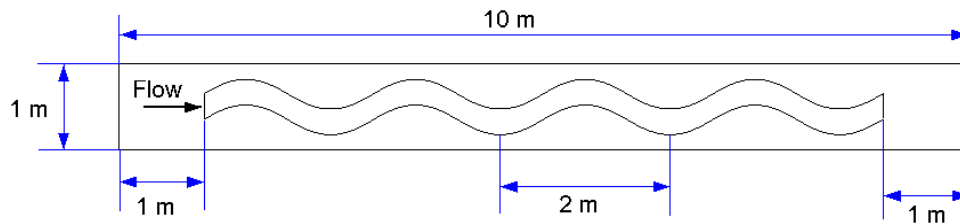
- (a) Time-average the toe shear stress, near-bank water elevation, toe vertical erosion, etc. over the duration of the bank time step and transfer these to each bank;
- (b) Distribute the shear stress along the wetted bank;
- (c) Perform combined basal erosion and mass failure computation using the analytical rate expression with the uniform retreat module, and skip the rest of the steps, (d) through (f); or
- (d) Perform basal erosion by computing the lateral erosion volume (actually area for the bank cross section) of the wetted bank;
- (e) Apply the lateral erosion volume to the cleanout tank first if not empty, and then apply to the wetted bank face (if any) and deform the bank accordingly; and
- (f) Check the geotechnical stability of the bank, update the new bank geometry if mass failure occurs, and add the failed blocks to the cleanout tank.

After all banks are simulated for bank retreat, the toe and top retreat distances are transferred back to the mobile-bed model. The 2D mesh is then moved and deformed to follow the new bank location. In addition, the sediment volume by size classes removed during the basal erosion step is added to the stream for transport by the mobile-bed model.

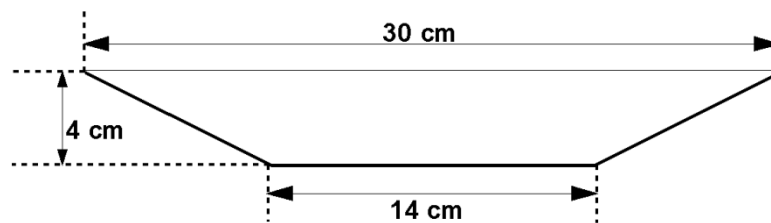
3.0 Model Verification

The bank erosion model is first verified with the uniform retreat module as described below. The mechanistic failure module has been verified before and may be found in the paper by Lai et al. (2012a).

The uniform retreat module, both the moving mesh and the fixed mesh versions, is verified using the laboratory meander cases of Nagata et al. (2000). The experiments were carried out in a tilting flume having length of 10 m, width of 1 m, and depth of 0.2 m. The initial meander channel was in the form of the sine-generated curve having wavelength of 2 m and maximum angle of 30 degree from the longitudinal direction (Figure 3). The channel cross section was trapezoidal and uniform along the channel initially; its dimensions are marked in Figure 3. Four channel wavelengths were used in the experiment, but data were measured only in the second from the the upstream. The numerical model simulates only the first three wavelengths since the results in the fourth do not impact the second.



(a) Plan Form

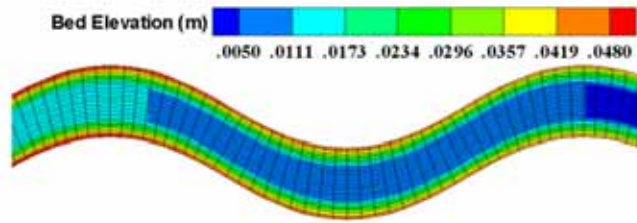


(b) Cross Section

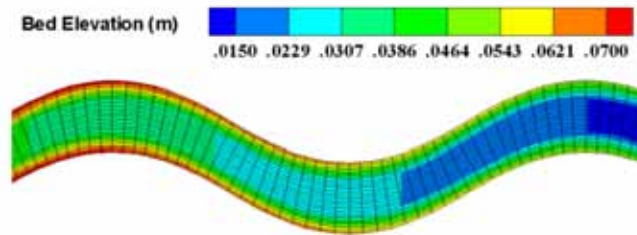
Figure 3. Flume configuration and initial meander channel form

Two simulation runs are carried out. Run 1 has a flow discharge of 1,980 cm³/s, initial bed slope of 1/300, and initial water depth of 3 cm; Run 3 has a flow discharge of 1,000 cm³/s, initial bed slope of 1/100, and initial water depth of 1.42 cm. Both the bed and bank consisted of fairly uniform sand with a mean diameter of 1.42 mm ($\sqrt{d_{84}/d_{16}} = 1.28$). Sediment was fed at the upstream end of the channel continuously in the experiments, and the channel evolution was initiated and the meander form was measured.

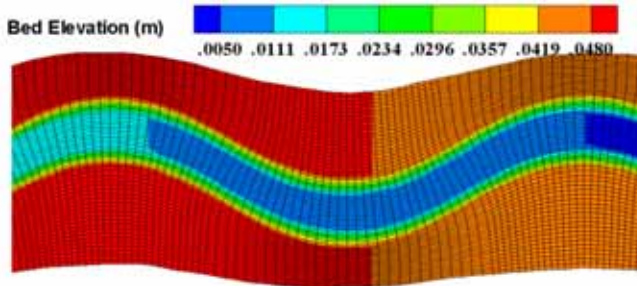
Both the moving and fixed mesh approaches are used for simulation. The moving mesh scenario has an initial mesh of 2,684 cells, consisting of 123 longitudinal points and 23 lateral points (Figure 4). This initial mesh is deforming while banks are retreating, but the total number of mesh cells and mesh topology remain unchanged throughout the simulation. Two fixed meshes are used: Run 1 uses a mesh of 5,612 cells and Run 3 has a mesh of 11,424 cells (see Figure 4). The fixed mesh approach needs more mesh cells due to accuracy concern as discussed before. Also, the solution domain needs to be larger than the moving mesh scenario to take into account potential bank retreat. Run 3 also tests sensitivity of mesh type and density.



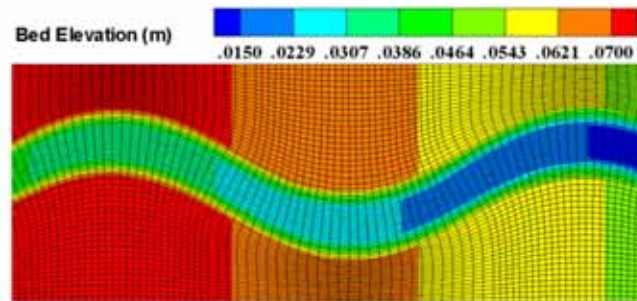
(a) Run 1 with Moving Mesh Method



(b) Run 3 with Moving Mesh Method



(c) Run 1 with the Fixed Mesh Method



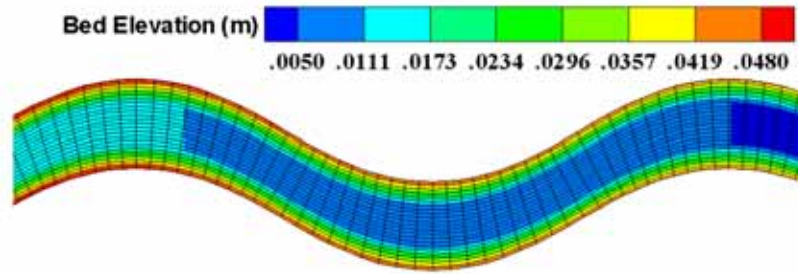
(d) Run3 with the Fixed Mesh Method

Figure 4. Initial meshes used for Run 1 and Run 3 using both the moving and fixed mesh approaches (contour represents the initial bed elevation)

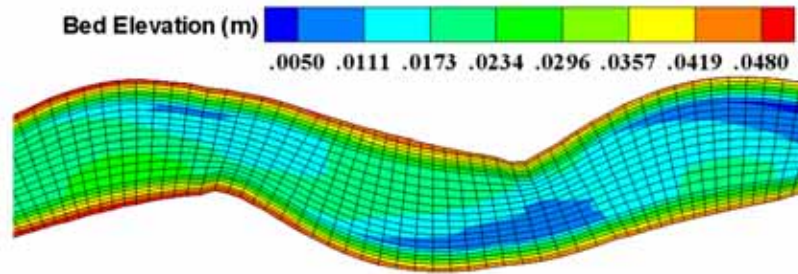
Model inputs include the following. The bed and bank are set to have uniform sand of a diameter of 1.42 mm. The upstream discharge is imposed as the boundary condition and the sediment feed rate is estimated using the Engelund and Hansen (1972) equation so that there is no net erosion or deposition at the upstream section. The only downstream boundary condition is the water elevation that is specified based on the measured data. The same Engelund and Hansen equation is used to compute the entrainment rate in the non-equilibrium sediment transport partial differential equation. The bedload adaptation length uses the Philip-Sutherland formula (1989) which was found suitable for sandy beds; and the active layer thickness is 10 times the sediment diameter. A uniform Manning's roughness coefficient of $n=0.0168$ is used; it is estimated using the grain shear stress expression $n = d^{1/6} / 20$ (d is the mean sediment diameter).

Both the left and right banks are simulated for retreat with the following bank properties. The critical shear stress is computed, by assuming the Shields number of 0.027, to be 0.62 Pa. The bank erodibility coefficient is calibrated and a value of $k = 2.0 \times 10^{-4} \text{ ms}^{-1}$ is found and used for all model runs. The initial bank slope is assumed to be maintained during bank retreat.

Model results with Run 1 are shown in Figure 5 and Figure 6. Figure 5 compares the initial mesh at $t=0$ and the final mesh at $t=125$ minutes, along with contours of bed elevation changes, for the moving mesh approach. Figure 6 compares the predicted bank retreat process, using both the moving and fixed mesh approaches, with the measured data. The results show that bank erosion starts at the downstream half of the outer bend and extends into the inner bend, while bar deposition occurs on the downstream half of the inner bend. The three sets of bank retreat results, two simulated and one measured, agree with each other in general trends of erosion locations and extent. There is some underprediction of the retreat rate and amount by both moving and fixed mesh approaches in the model results relative to measured data.

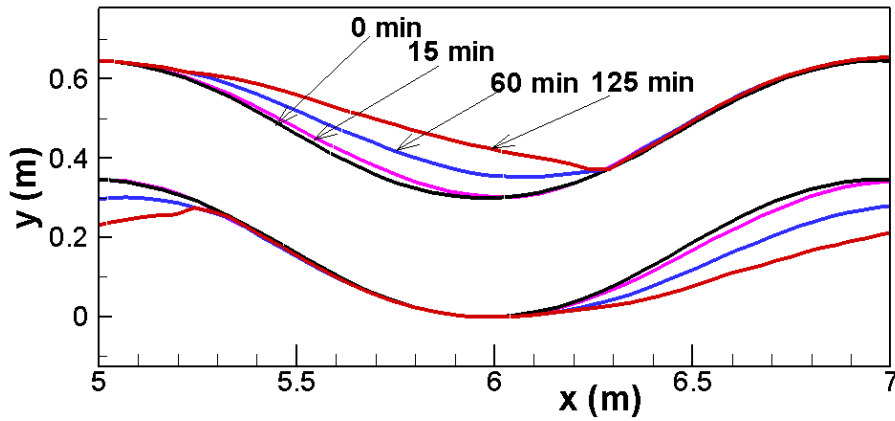


(a) $t = 0$ minute

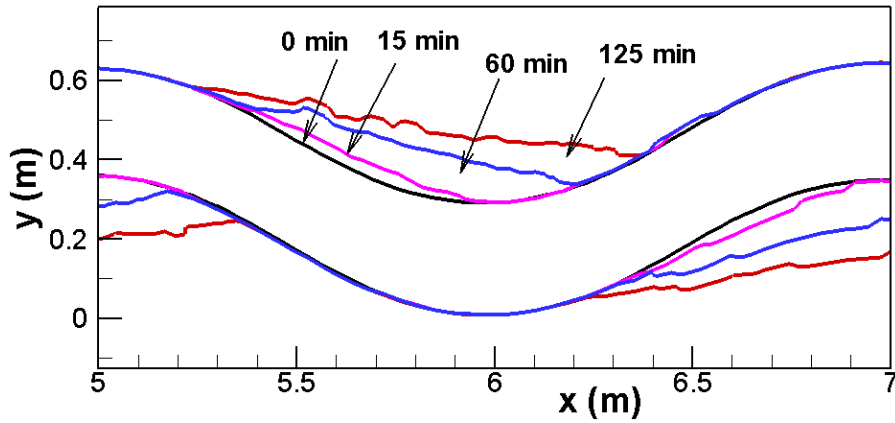


(b) $t = 125$ minutes

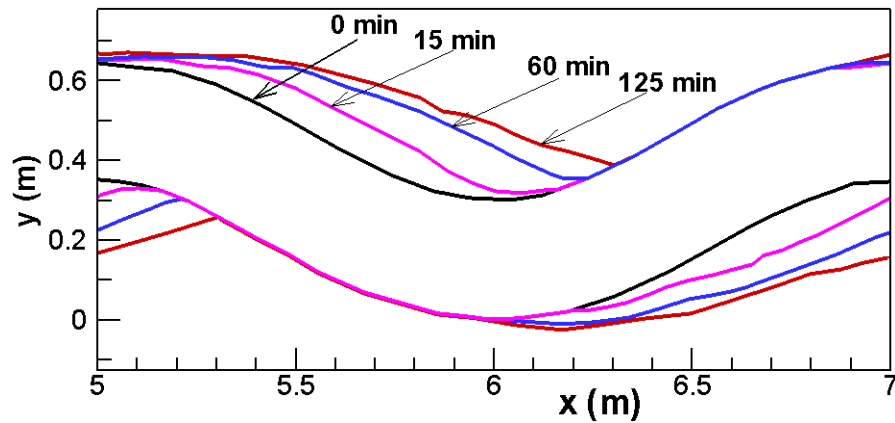
Figure 5. Initial and final meshes for Run 1 with the moving mesh (contours are bed elevation)



(a) Prediction with the Moving Mesh



(b) Prediction with the Fixed Mesh

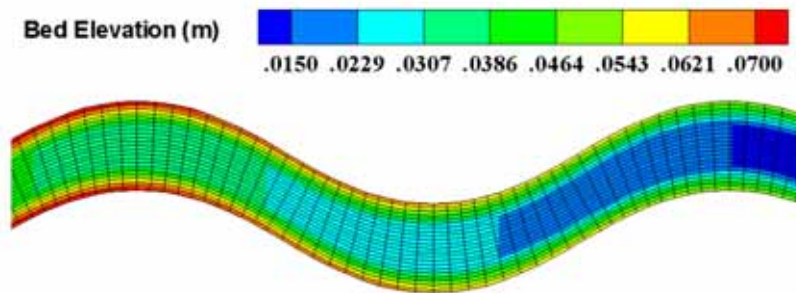


(c) Measured data

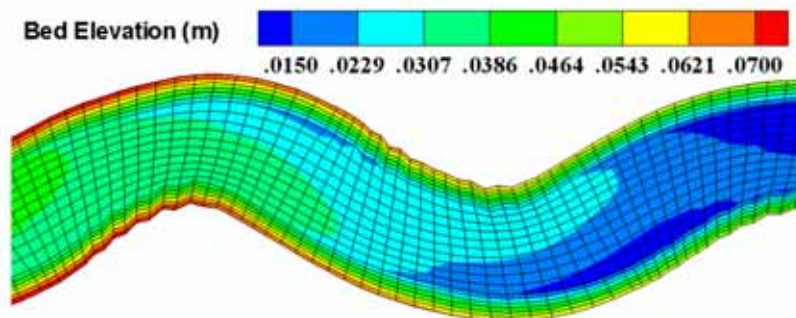
Figure 6. Comparison of predicted and measured bank retreat for Run 1

Model results with Run 3 are shown in Figure 7 through Figure 9. The meshes in Run 1 and 3 were generated with quadrilateral elements. An additional mesh, a mixed mesh

having 10,944 quadrilateral and triangular mesh cells, is added for the Run 3 moving mesh simulation in order to test the mesh type sensitivity of the model. Figure 7 and Figure 8 compare the initial meshes at $t=0$ and the final meshes at $t=110$ minutes for the two moving meshes, along with changes of the bed elevation. Figure 9 compares the predicted bank line retreating process with the measured data with both the moving and fixed meshes. The results show that the predicted bank retreat of all numerical models agrees with the measured data reasonably well. Similar to Run 1, the predictions have a slightly slower rate and extent of total bank erosion compared to measured data. Different meshes produce very similar results, which indicates that the errors introduced by the mesh type and mesh density are relatively small with the meshes adopted. Also, both the moving and fixed mesh approaches predict similar bank retreat results despite their vastly different methodologies used. This demonstrates that both approaches are implemented correctly, and the procedure developed for each approach works well.

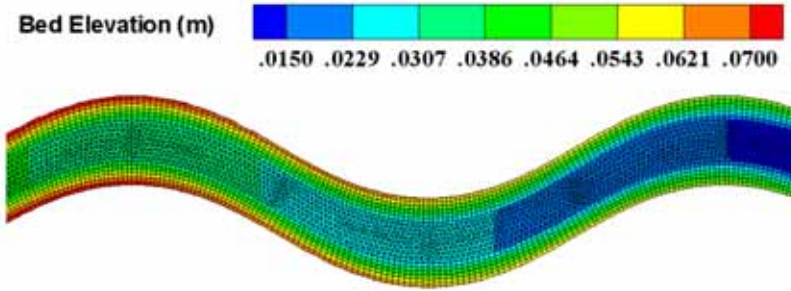


(a) $t = 0$ minute

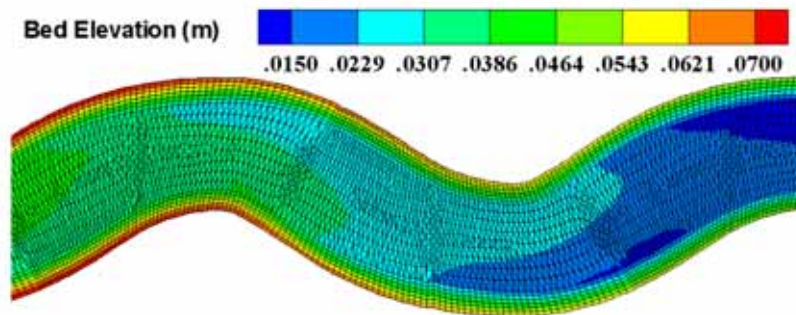


(b) $t = 110$ minutes

Figure 7. Initial and final meshes for Run 3 with the moving mesh (contours are bed elevation)

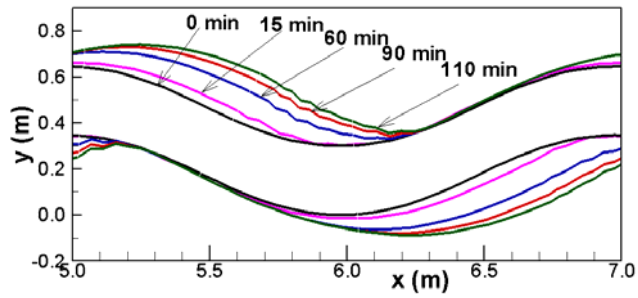


(a) $t = 0$ minute

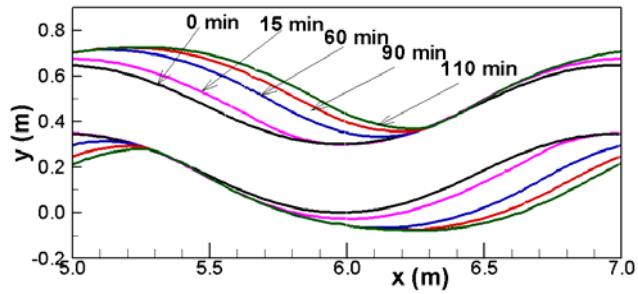


(b) $t = 110$ minutes

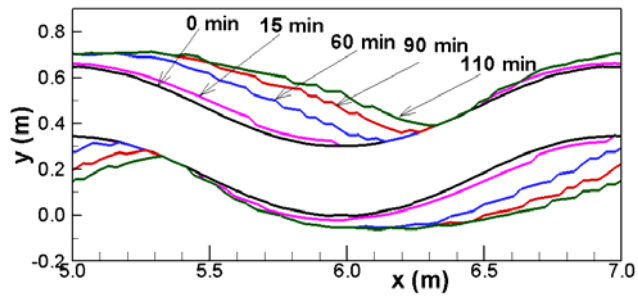
Figure 8. Initial and final meshes for Run 3 with the mixed, moving mesh (contours are bed elevation)



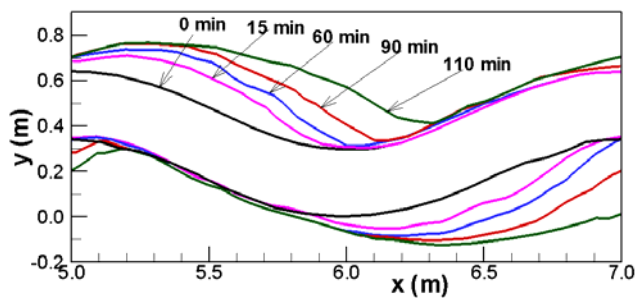
(a) Prediction with the Quadrilateral Moving Mesh



(b) Prediction with the Mixed Moving Mesh



(c) Prediction with the Fixed Mesh



(d) Measured data

Figure 9. Comparison of predicted and measured bank retreat for Run 3

4.0 Results with Glines Canyon Dam Removal Physical Model Scenario

In this section, SRH-2D with bank erosion modules is applied to simulate the delta erosion and deposition processes during Glines Canyon Dam removal at the physical model scale. The model setup and results are described.

4.1 About the Physical Model Test

The physical model test of the Elwha Dam removal was carried out by Chris Bromley (2007). The physical model test scaling and parameters are listed below:

- It is a distorted model in order to minimize surface tension issue. The prototype to model scale in the horizontal plane is 1:310, while the vertical scale is 1:81.7. Or, they can be written as:

$$L_r = \frac{L_p}{L_m} = \frac{3,300}{10.65} = 310; \quad Y_r = \frac{Y_p}{Y_m} = \frac{48.77}{0.597} = 81.7$$

- The flow discharge of the model is computed as:

$$Q_m = Q_p \times X_r^{-1} Y_r^{-1.5} = \frac{59.4}{310 \times 81.7^{1.5}} = 0.000259 \text{ m}^3/\text{s}$$

This equates to $Q_m \times 60,000 \text{ litres/min.} = 15.57 \text{ litres/min.}$

- Channel Slope: $S_m = S_p \times X_r Y_r^{-1} = 0.017 \times \frac{310}{81.7} = 0.065$
- Friction coefficient: $C_{f_m} = C_{f_p} \times X_r Y_r^{-1} = 0.01 \times \frac{310}{81.7} = 0.038$
- Discharge per unit channel width: $q_{w_m} = q_{w_p} \times Y_r^{-1.5} = \frac{2.29}{81.7^{1.5}} = 0.0031 \text{ m}^2/\text{s}$
- Flow depth: $H_m = H_p \times Y_r^{-1} = \frac{0.68}{81.7} = 0.0083 \text{ m}$
- Froude number: $Fr_m = \left(\frac{q_{w_m}^2}{g_m H_m^3} \right)^{0.5} = \left(\frac{0.0031^2}{9.81 \times 0.0083^3} \right)^{0.5} = 1.30$
- Shields number: $\tau_m^* = \frac{H_m S_m}{R_m D_{50m}} = \frac{0.0083 \times 0.065}{1.65 \times 0.000557} = 0.584$

- The time required for one week of prototype flow time (in seconds) to occur in the model is: $T_m = T_p \times \frac{Y_r^{0.5}}{X_r} = 604,800 \times \frac{81.7^{0.5}}{310} = 4.9$ hours ,
- The time required for one week of prototype sediment transport to occur in the model is: $T_m = T_p \times \frac{Y_r^2}{X_r^{2.5}} = 604,800 \times \frac{81.7^2}{310^{2.5}} = 0.66$ hours.

The geometrical hydraulic variables are summarized in Table 1.

Table 1. Prototype and model geometrical hydraulic variables

Parameter	Prototype value	Prototype data source	Model value	Scale ratio/equation
Reservoir length (straight line from mouth of Rica Canyon to dam)	3.3 km	USGS (2000)	10.65 m	X_r
Maximum reservoir width	1.067 km	USGS (2000)	3.44 m	X_r
Effective vertical geomorphological range	48.8 m	(Bureau of Reclamation, 1995b)	0.597 m	Y_r
Delta length	1,000 m	USGS (2000)	3.23 m	X_r
Maximum delta width	400 m	USGS (2000)	1.29 m	X_r
Increments of baselevel drop	2.29 m	(Bureau of Reclamation, 1996a)	0.028 m	Y_r
Mean channel width (Entrance Channel???)	25.91 m	USGS (2000)	0.084 m	X_r
Bed slope (S)	0.017	(Bureau of Reclamation, 1996b)	0.065	Y_r / X_r
Channel friction coefficient (C_f)	0.01	Estimated (Parker, Written Communication, 2003)	0.038	$C_{f_r} = \frac{Y_r}{X_r}$
Discharge (Q)	59.4 m ³ s ⁻¹	(Bureau of Reclamation, 1996b)	15.57 l/min	$Q_r = X_r Y_r^{1.5}$
Discharge per unit width (q_w)	2.29 m ² /s	$q_w = Q / B$	0.0031 m ² /s	$q_{w_r} = Y_r^{1.5}$
Flow depth (H)	0.68 m	$H = \left(\frac{C_f q_w^2}{gS} \right)^{1/2}$	0.0083 m	$H_r = Y_r$
Froude number (Fr)	1.3	$Fr = \left(\frac{q_w^2}{gH^3} \right)^{0.5}$	1.3	$Fr_m = \left(\frac{q_{w_m}^2}{g_m H_m^3} \right)^{0.5}$
Shields number (τ^*)	0.584	$\tau^* = \frac{HS}{RD_{50}}$	0.584	$\tau_m^* = \frac{H_m S_m}{R_m D_{50m}}$
Flow time (T_f)	1 week	-	4.9 hours	$T_r = \frac{X_r}{Y_r^{0.5}}$
Sediment transport time (T_s)	1 week	-	0.66 hours	$T_{s_r} = \frac{X_r^{2.5}}{Y_r^2}$

The initial model basin for the physical model test was constructed from a pre-dam geometry as shown in Figure 10.

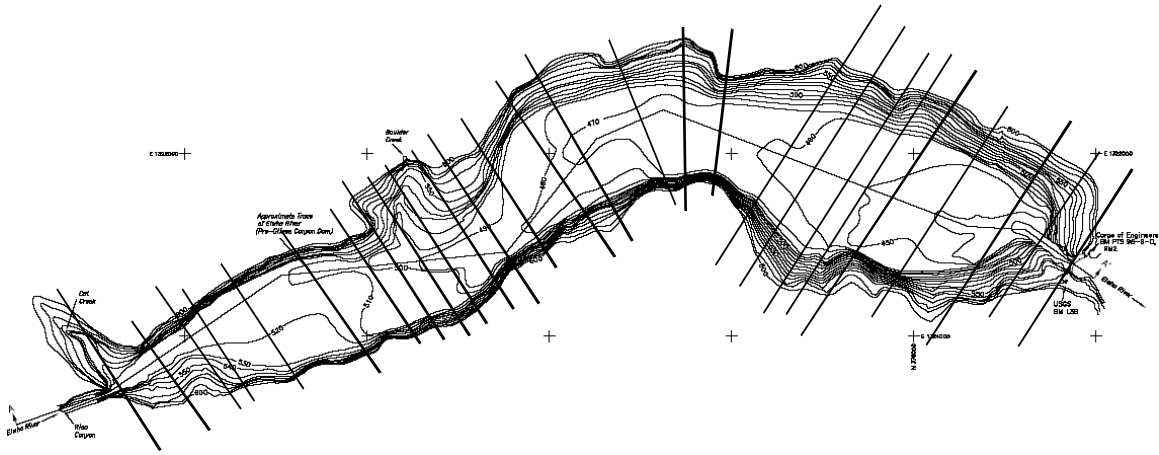


Figure 10. Contour map of pre-dam Elwha River valley showing locations of model construction cross-sections

The physical model test has been described in detail by Bromley (2007). A brief description is provided below:

- Each experiment was started by hydraulically growing the model delta to the same extent as the 2002 prototype delta, although no attempt was made to try and recreate the bottomset deposits (e.g. lakebed muds). Dam removal was accomplished by pulling “notches” out of the downstream model boundary to represent multiple reservoir drawdown increments.
- The dam removal phase of each experiment was performed using a constant discharge of 15.57 litres per minutes, which scales to a prototype discharge of 59.4 m³/s (2,098 cfs) and is close to the values under which the prototype is planned to be removed (Reclamation 1996).
- The removal of each dam increment was also performed so that the reservoir water surface elevation fell at the same rate of 2.8 cm per 15 minutes.
- Following the removal of each dam increment, the delta surface channel system was allowed to adjust until virtually all sediment transport had ceased, i.e. until a static equilibrium condition was attained, which was defined as the slow movement of only a few sand grains along the channel bed, at which point the next dam increment was removed. It was possible to reach a static equilibrium since each run was performed without a sediment feed.
- In most runs in which the dam was completely removed, one or several flood flows were run through the model once the delta surface channel system had reached a static equilibrium condition following the removal of the last dam increment. Scaled two- and five-year return interval flows were used, since these

have a statistically very good chance of occurring during or shortly after the dam removal period.

- During the periods of system relaxation during the dam removal phase of each run, the model's discharge was switched off and the reservoir drained at intervals of 1.5, 3.5, 5.5 and 9.5 hours of run time, and sometimes at additional intervals in between, in order to scan the entire delta surface and record topographic measurements.

4.2 Case 3xC Scenario

A specific model run, 3xC, was selected for SRH-2D model test and validation in this study. This corresponds to the central pilot channel scenario in which three notches were removed for each model run. Figure 11 shows the delta terrains at time 0 and time 220 minutes during the physical model test. In the physical model, the flow was run at a constant discharge of $260 \text{ cm}^3/\text{s}$ and the initial delta was formed. After the equilibrium is reached, three notches were suddenly removed (this is called time zero in this study) and delta evolution was then initiated.

Our numerical modeling intends to replicate the physical model delta erosion processes that includes significant lateral erosion for the center pilot channel scenario.

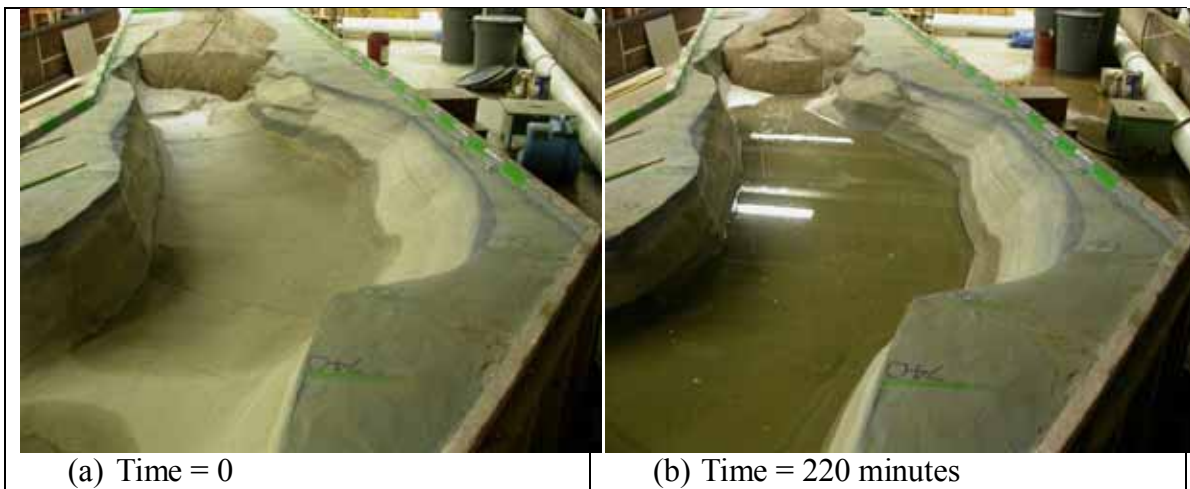


Figure 11. Initial terrain and terrain after 220 minutes during the physical model test

The numerical model was constructed initially from an empty basin (EB) terrain similar to the way done for the physical model. The bed elevation of the EB terrain is displayed in Figure 12(a). An initial delta, based on the physical model measured terrain, was then added to the EB terrain to form the initial delta (ID) terrain (see Figure 12b). Further, the entrance channel into the reservoir and the central pilot channel were also added in the numerical modeling study, the same way as the physical model. The entrance channel is 50 cm long and 8.34-8.4 cm wide, and has a slope of 0.0645. The initial terrain through the delta for the 3xC case is displayed in Figure 13 and it is used by the numerical model as the initial condition. This initial terrain closely matches the terrain used by the physical

model. The ID terrain with the pilot channel added was used as the initial model terrain for both physical and numerical models.

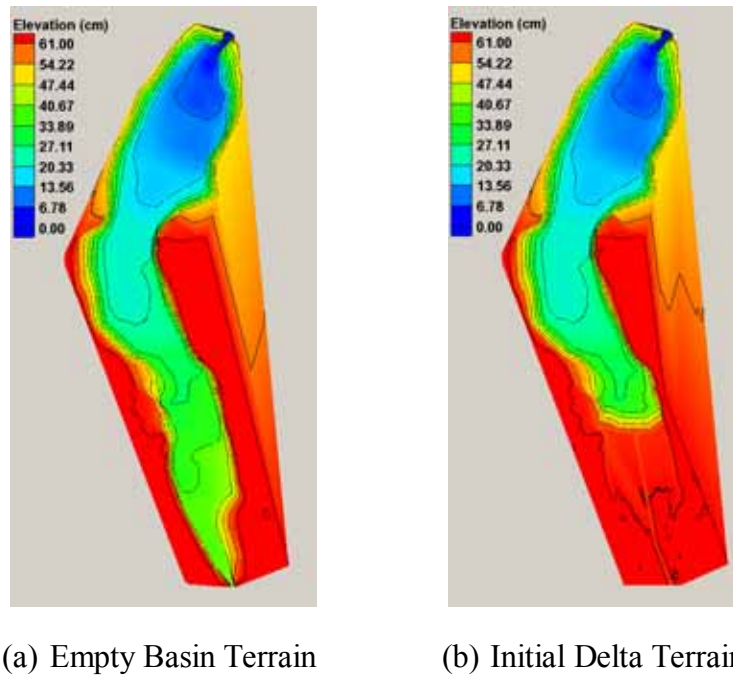


Figure 12. Contours of the empty basin terrain and the initial delta terrain used for both numerical and physical models

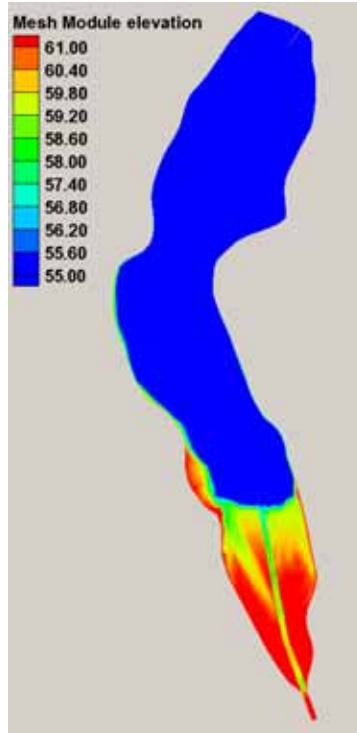


Figure 13. Contours of the initial delta terrain used for the numerical modeling; note the entrance channel and the pilot channel added to the delta. Note that all elevations below 55 are shown as blue to emphasize topography in delta section.

4.3 Other Model Details

With SRH-2D modeling, a 2D solution domain and a mesh are developed first and they are shown in Figure 14. The Lake Mills mesh consists of 6,005 quadrilateral cells and 6,091 nodes.

Flow simulation input parameters include mainly the flow roughness coefficient, the flow rate through the reservoir and the downstream water elevation. For the 3xC case simulated, a constant Manning's roughness coefficient of 0.027 is used estimated for sandy bed with medium diameter of 0.43 mm. The flow discharge into the reservoir is 260 cm³/s (physical model scale), while the downstream water elevation is maintained at 51.6 cm according to the measured elevation after three notches removed.

The prototype delta in Lake Mills was composed of 23.7% clay and silt, 61.4% sand, 14.2% gravel and 0.7% cobble and boulder as measured by field studies. The prototype delta sediment gradation was coarser at the surface and became finer in gradation closer to the bottom. The delta sediment mixture utilized in the physical model is simplified from the field measurements. Numerical modeling is based on the physical model mixture. The numerical model divides the sediment mixture of the delta into eight (8) size classes as shown in Table 2 and the delta mixture gradation was from the measured data in the physical model shown in Figure 15. The medium diameter is about 0.43 mm.

The transport of each size class is governed by a differential equation with its erosional capacity rate computed by the Eugeland-Hansen formula. The sediment transport is treated as bedload and the adaptation length is based on the Sutherland-Philip equation. The active layer thickness is assumed to be a constant value of 3 cm. The thickness of the delta is another input that is easily obtained by the elevation difference between the delta terrain and the empty basin terrain shown in Figure 12.

Pilot channel evolution was simulated with the bank erosion module coupled with the regular 2D vertical erosion simulation as described above. The three bank lines, left, right and center, were used to define the bank erosion zone as shown in Figure 15. The left to center lines define the zone of left bank potential erosion while the center to right lines define the zone of right bank erosion. The input parameters for bank erosion module include the critical shear stress, erodibility, angle of repose in the wetted bank, and toe and top locations. In this simulation, the critical shear stress was estimated to be 0.36 Pa, while the erodibility was calibrated to be 1.0e-5. The angle of repose for wetted portion of the bank was set at 15 degree.

Table 2. Sediment size classes within the initial delta with the numerical model

Size(mm)	.05-.125	.125-.25	.25-.355	.355-0.5	0.5-1	1-2	2-4	4-10
----------	----------	----------	----------	----------	-------	-----	-----	------

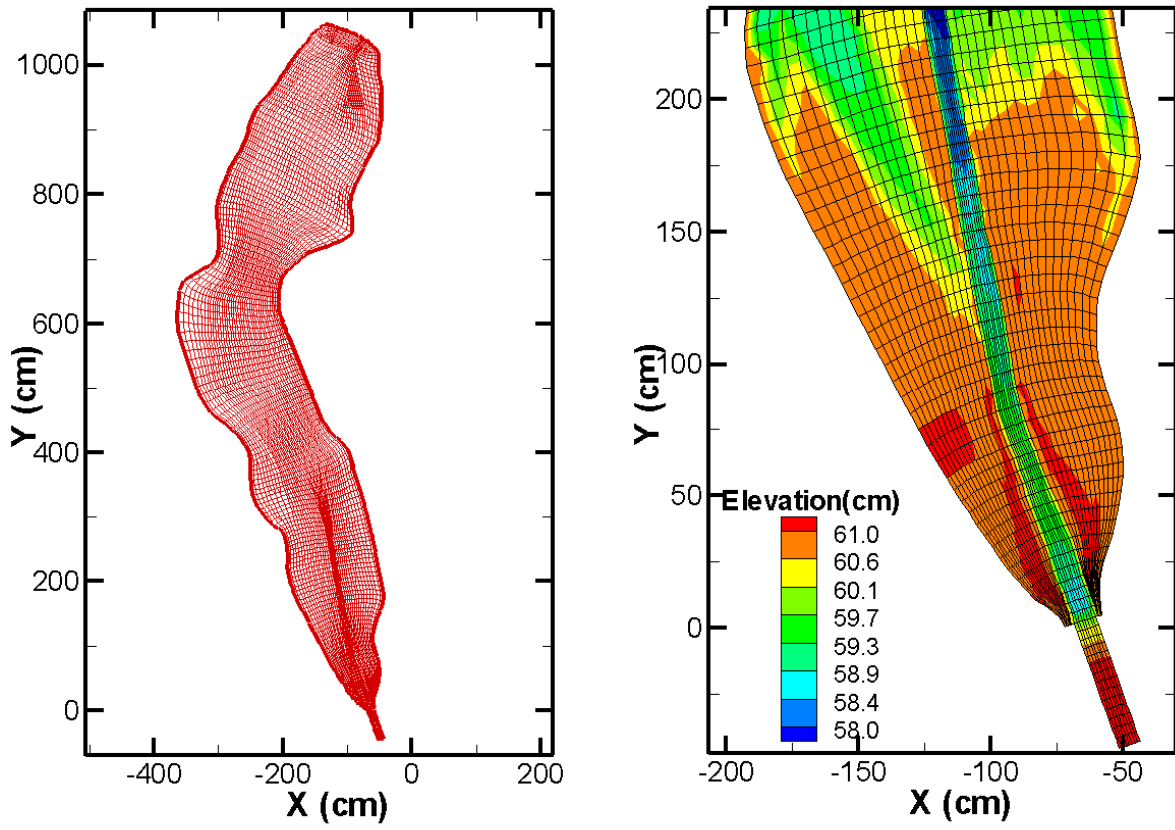


Figure 14. Solution domain and mesh used for the simulation

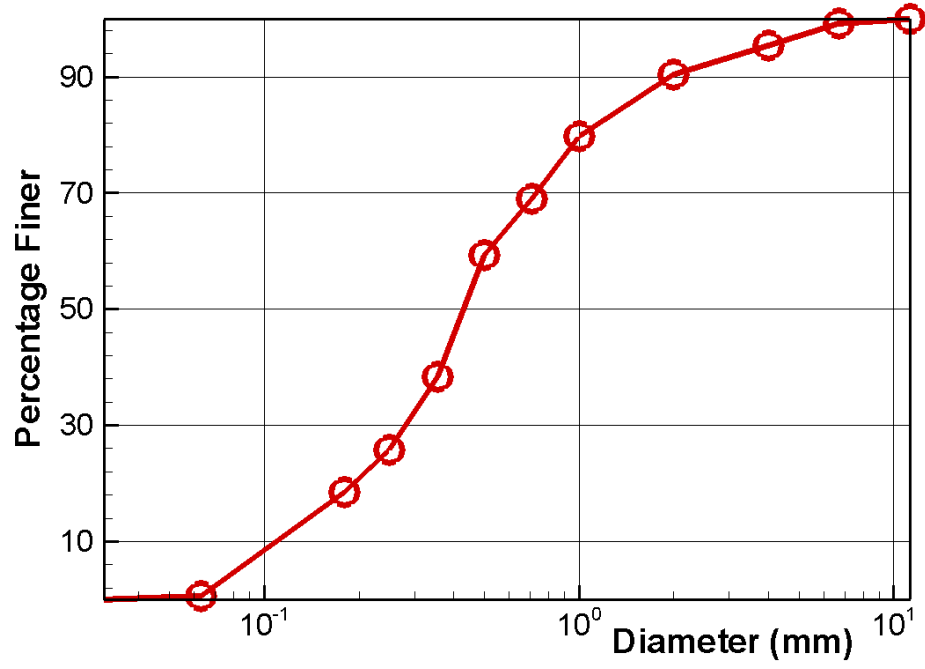


Figure 15. Initial sediment gradation of the delta in the physical model test

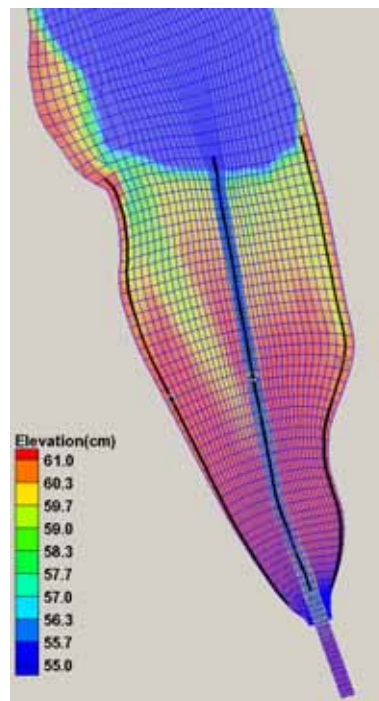


Figure 16. Three boundary lines (shown in black) used to define bank erosion zones

4.4 Model Results

First, a flow-only model run at $260 \text{ cm}^3/\text{s}$ was carried out without sediment transport or dam removal. The model run results are used as the initial flow condition for the delta evolution model run. The initial terrain of the 3xC case is shown in Figure 17 with bed elevation contours displayed. The predicted equilibrium flow velocity and water depth fields are displayed in Figure 18. Near the basin entrance, the flow is mostly contained within the pilot channel having the highest velocity. Near the dam notch, flow is nearly stagnant.

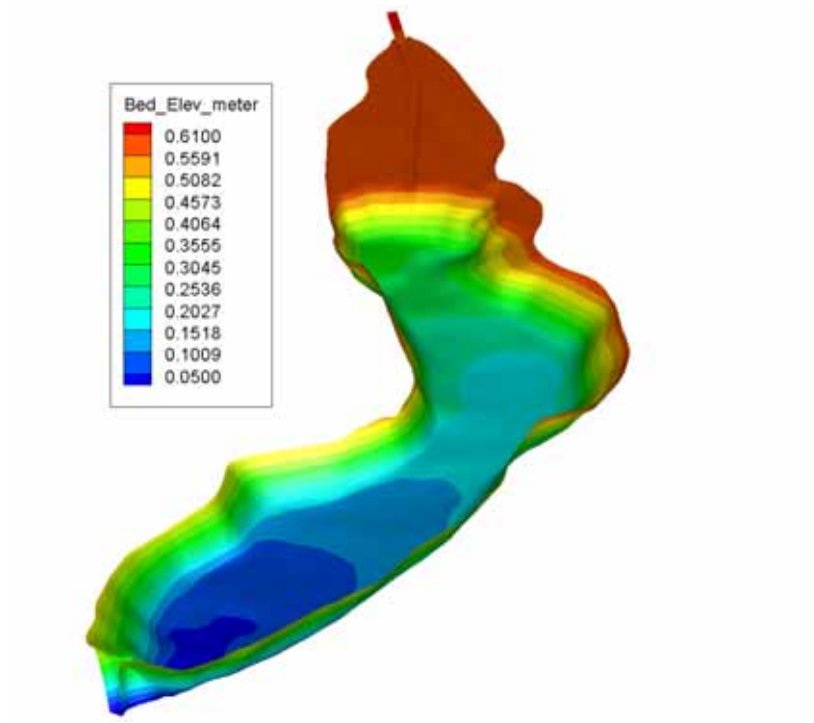


Figure 17. 3D view of the initial geometry of the 3xC case

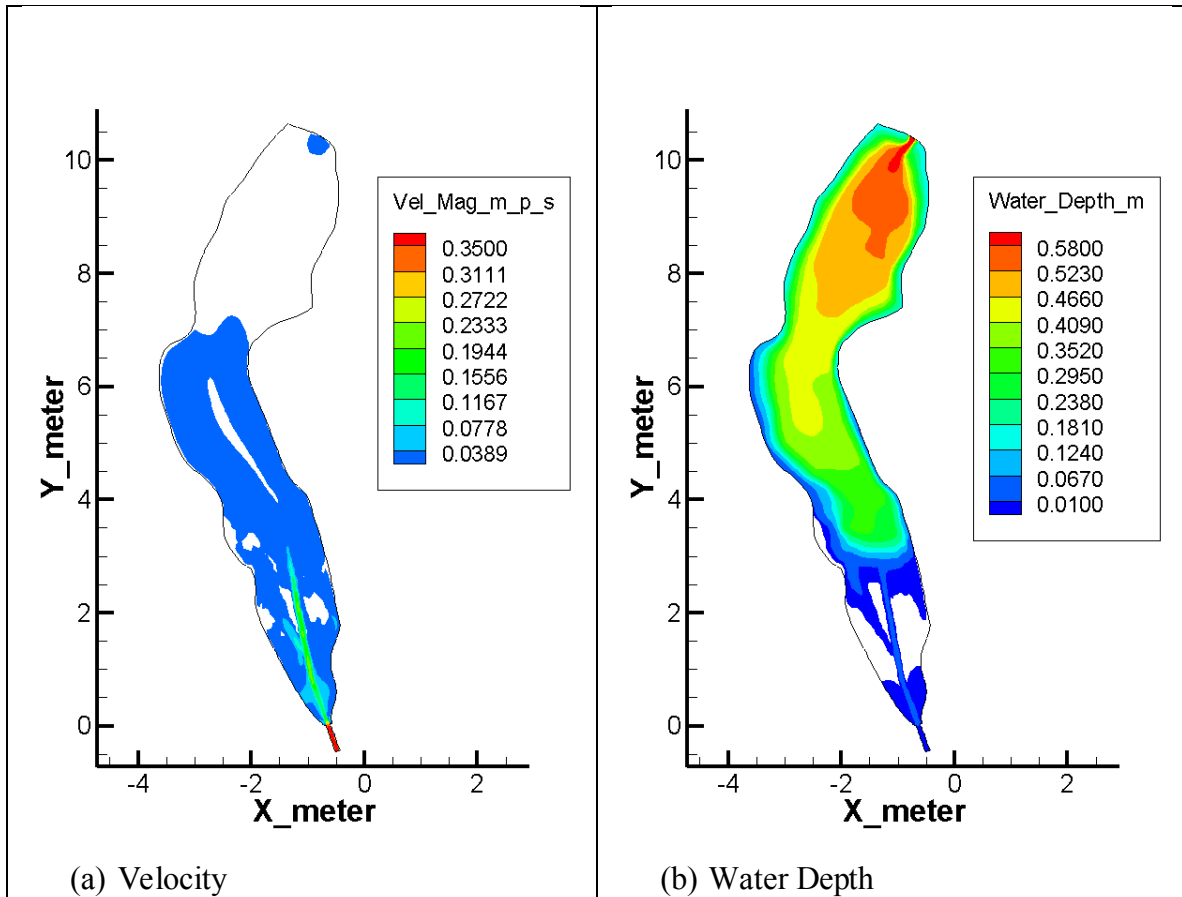


Figure 18. Predicted flow velocity and water depth for the flow-only model run (blank area in velocity plot is the almost still water area)

Next, a sediment transport simulation is carried out starting from the flow conditions obtained with the flow-only modeling and no dam removal. The purpose of the run is to gain an understanding of the erosion and deposition characteristics of the delta before the dam is removed, lowering the base level. The simulated net erosion and deposition results after equilibrium are localized to two small spatial areas that overall have negligible effects on the delta topography (Figure 19). This is consistent with the physical model results of the initial delta terrain and gradation obtained after equilibrium had been reached.

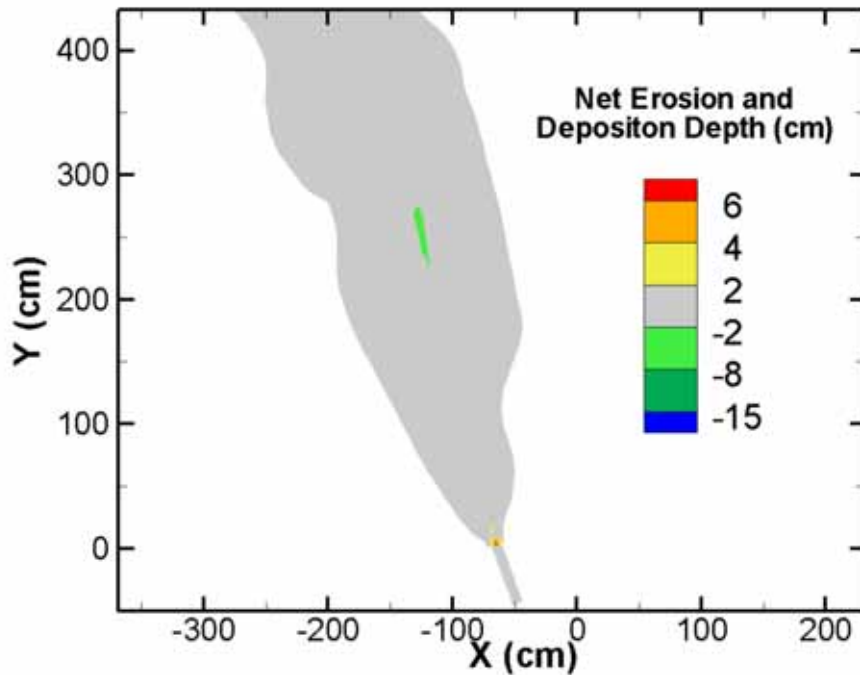


Figure 19. Predicted erosion and deposition depth (cm) of the delta when no dam removal is performed

Finally, simultaneous vertical and lateral erosion geofluvial simulation is carried out for 12 hours after the sudden removal of the first 3 notches of the dam. The time step used for the simulation is 0.2 seconds. After sudden removal of three dam notches, the downstream water elevation is lowered, flow velocity on the delta is increased, and delta erosion and deposition processes are initiated. The predicted delta evolution at different times is shown in Figure 20. It is seen that the pilot channel experiences immediate vertical erosion, and as a result, both left and right banks are eroded and collapsed. The simultaneous vertical and lateral erosion process occurs for more than 10 hours, eventually reaching equilibrium.

The predicted net erosion and deposition thickness after 220 minutes following the sudden 3-notch removal (Figure 21(a)) is compared with the physical model measurements (Figure 21(b)). Further, the same numerical model is run but without the bank erosion module turned on; this result is displayed in Figure 22. Based on these results, we can observe the following:

- Without the bank erosion module, the model can only predict the vertical erosion of the pilot channel; no lateral erosion will be predicted by the model.
- With the vertical bank erosion module turned on, the SRH-2D is capable of predicting simultaneous vertical and lateral delta erosion.

- Overall, SRH-2D predicts the qualitative delta erosion and deposition satisfactorily. For example, the model predicts that the pilot channel will shift to the right despite that it is the left bank that experiences higher shear stress at the beginning due to the slight curving towards the left. This right bank shift is also observed in the physical model.
- However, the model predicts too much bank erosion in the upstream half of the pilot channel, which is not observed by the physical model results. Also, the model still misses some of the erosion details.

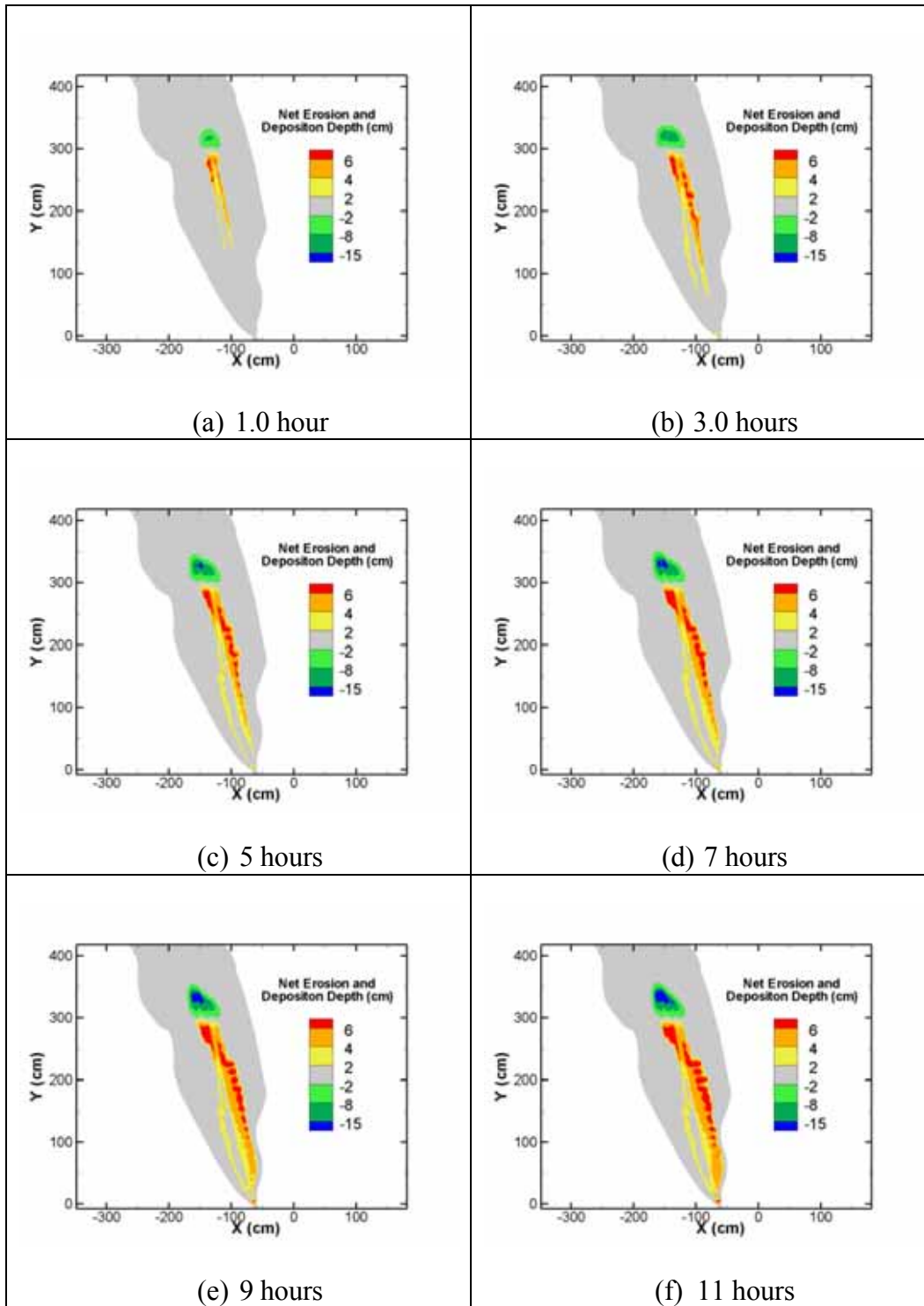
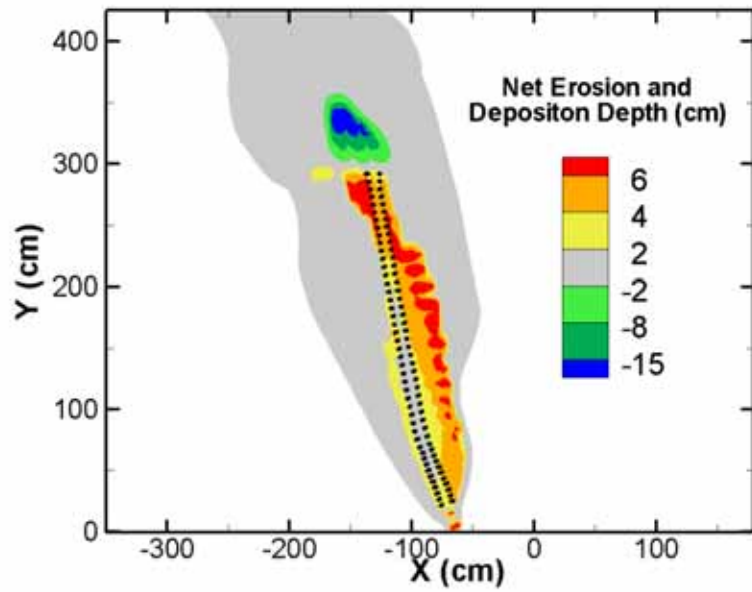
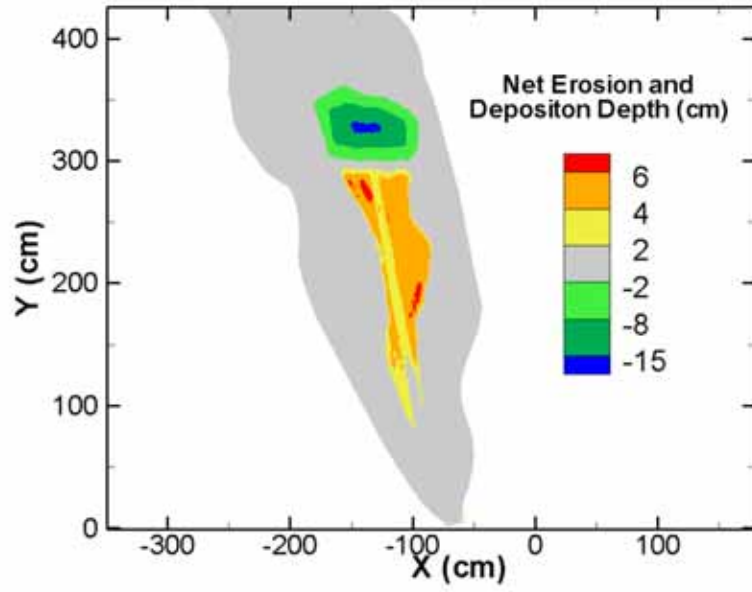


Figure 20. Simulated delta evolution to equilibrium



(a) Model Prediction



(b) Physical Model Measurement

Figure 21. Comparison of predicted (black dots are locations of the initial pilot channel) and measured erosion and deposition depth (cm) when the delta reached equilibrium after removal of 3 notches

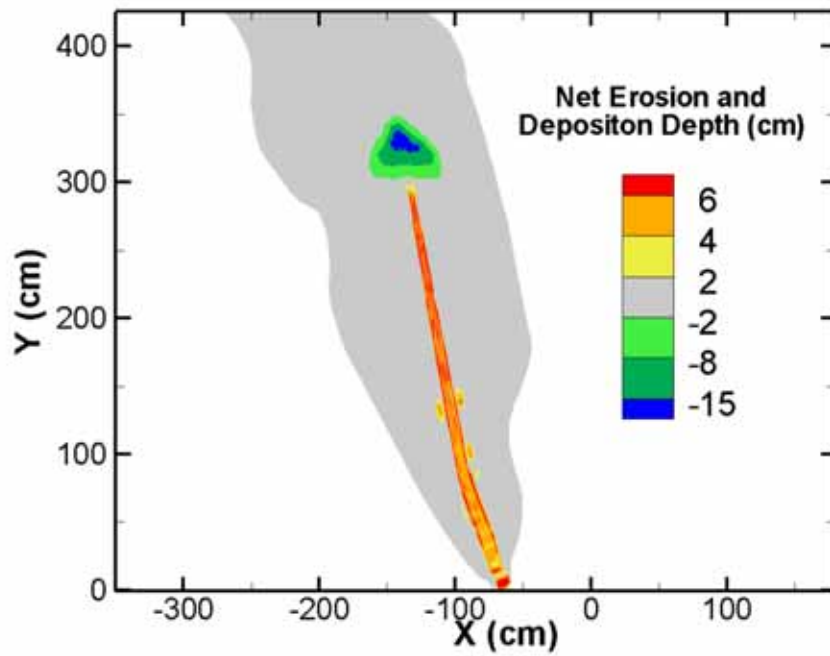


Figure 22. Predicted erosion and deposition depth (cm) when the delta reached equilibrium after removal of 3 notches without bank erosion module turned on

5.0 Concluding Remark

The objective of the current research is to find out whether the existing SRH-2D model is capable of predicting simultaneous vertical and lateral sediment erosion and deposition processes upstream of the dam during dam removal. In particular, SRH-2D model, which coupled bank erosion modules with the mobile-bed model, is used to simulate the delta erosion and deposition characteristics when dam notches are removed in the physical model of Elwha Dam removal. The study finds that the improved SRH-2D is capable of simulating simultaneous vertical and lateral erosion of the delta processes during dam removal. For example, qualitative erosion and deposition patterns are well predicted by the model. Comparison with model simulation without lateral bank erosion demonstrates that the predicted erosion pattern is predicted totally wrong if lateral erosion component is not taken into account.

The research, however, finds that some of the details of the delta erosion are missed by the improved SRH-2D model. For example, predicted erosion at the upstream half of the pilot channel is not observed in the physical model. It is further found that the bank erosion modules implemented in SRH-2D still have limitations in that the model may fail if the bank toe point is moving significantly in the vertical direction.

It is recommended that further research and development are needed in the future. New bank module needs to be developed that can track the bank toe point in a robust and stable way.

6.0 References

- Bromley, J.C. (2007). *The Morphodynamics of Sediment Movement through a Reservoir during Dam Removal*. Ph.D. Thesis, the University of Nottingham,
- Engelund, F., and Hansen, E. (1972). *A monograph on sediment transport in alluvial streams*. Teknisk Forlag, Technical Press, Copenhagen, Denmark.
- Greimann, B.P., Lai, Y.G., and Huang, J. (2008). "Two-Dimensional Total Sediment Load Model Equations." *J. Hydraul. Eng.*, 134(8), 1142-1146.
- Lai, Y.G. (2008). *SRH-2D Theory and User's Manual version 2.0*. Technical Service Center, Bureau of Reclamation, Denver, CO.
- Lai, Y.G. (2010). "Two-Dimensional Depth-Averaged Flow Modeling with an Unstructured Hybrid Mesh." *J. Hydraul. Eng.*, 136(1), 12-23.
- Lai, Y.G. (2013). *A Coupled Stream Bank Erosion and Two-Dimensional Mobile-Bed Model*. Technical Report No. SRH-2013-07, Technical Service Center, Bureau of Reclamation, Denver, CO.
- Lai, Y.G., and Greimann, B.P. (2008). *Two-Dimensional Numerical Model Study of Sediment Movement at the Robles Diversion Dam on the Ventura River, California*. Technical Service Center, Bureau of Reclamation.
- Lai, Y.G., and Greimann, B.P. (2010). "Predicting contraction scour with a two-dimensional depth-averaged model." *J. Hydraulic Research*, 48(3), 383-387.
- Lai, Y.G., and Przekwas, A.J. (1994). "A Finite-Volume Method for Fluid Flow Simulations with Moving Boundaries." *Computational Fluid Dynamics*, 2, 19-40.
- Lai, Y.G., Greimann, B.P., and Wu, K. (2011). "Soft bedrock erosion modeling with a two-dimensional depth-averaged model." *J. Hydraul. Eng.*, 137(8), 804-814.
- Lai, Y.G., Greimann, B.P., and Wu, K. (2012). "Modeling Bank Erosion in Fluvial Channels." *2012 River Flow.*, September 3-8: Costa Rica
- Lai, Y.G., Thomas, R., Ozeren, Y., Simon, A., Greimann, B.P., and Wu, K. (2012). "Coupling a Two-Dimensional Model with a Deterministic Bank Stability Model." *ASCE World Environmental and Water Resources Congress.*, Albuquerque, New Mexico, May 20-24.
- Lai, Y.G., Thomas, R., Ozeren, Y., Simon, A., Greimann, B.P., and Wu, K. (2014). "Modeling of multi-layer cohesive bank erosion with a coupled bank stability and mobile-bed model."

Geomorphology.

- Lai, Y.G., Weber, L.J., and Patel, V.C. (2003). "Non-hydrostatic three-dimensional method for hydraulic flow simulation - Part I: formulation and verification." *J. Hydraul. Eng.*, 129(3), 196-205.
- Langendoen, E.J., and Simon, A. (2008). "Modeling the evolution of incised streams. II: Streambank erosion." *J. Hydraul. Eng.*, 134(7), 905-915.
- Nagata, N., Hosoda, T., and Muramoto, Y. (2000). "Numerical analysis of river channel processes with bank erosion." *J. Hydraul. Eng.*, 126(4), 243-252.
- Phillips, B. C., and Sutherland, A. J. (1989). "Spatial lag effects in bedload sediment transport." *J. Hydraul. Res.*, 27(1), 115-133.
- Reclamation, B. o. (1996). *Sediment Analysis and Modeling of the River Erosion Alternative*. Elwha Technical Series PN-95-9, Bureau of Reclamation Technical Service Center, Denver, CO and Pacific Northwest Regional Office, Boise, ID, Denver, CO. 157 pp